



Tekirdağ Namık Kemal University
Çorlu Engineering Faculty
Textile Engineering Department



ICONTEX 2019

2nd INTERNATIONAL CONGRESS OF INNOVATIVE TEXTILES



PROCEEDINGS

17-18 April 2019

www.icon2019.org



International Congress of Innovative Textiles ICONTEx (17-18.04.2019)

ISBN

TK NO: 978-605-4265-58-9

Vol. 2: 978-605-4265-60-2

No part of this publication may be reproduced, stored in retrieval system or transmitted in any form or by any means, electronically, mechanical, photocopying, recording or otherwise, without the prior written permission of publisher, Tekirdağ Namık Kemal University.

No responsibility is assumed by the publisher for any injury and/or damage to persons or property as a matter of products liability, negligence or otherwise or form any use or operation of any methods, products, instructions or ideas contained in the material here in.



Organising Committee

Prof. Dr. Fatma GÖKTEPE

Chairperson of Organising Committee

Prof. Dr. Rıza ATAV

Member of Organising Committee

Prof. Dr. Pelin GÜRKAN ÜNAL

Secretary of Organising Committee

Res. Asst. Volkan YALI

Member of Organising Committee

Advisory Board*

Prof. Dr. Mümin ŞAHİN, Rector of Tekirdağ Namık Kemal University (Honorary President)

Fahrettin AKÇAL, Tekirdağ Provincial Director of Science Industry and Technology

Halil AKSOY, Denge Kimya ve Tekstil San. Tic. A.Ş.

Özgür AVCU, DMS Dilmenler Makine ve Tekstil San. Tic. A.Ş.

Vehbi CANPOLAT, Chairman of the Board of Textile Finishing Manufacturers Association of Turkey

Mehmet ÇİĞDEM, Yünsa Yünlü San. ve Tic. A.Ş.

Nuri DÜZGÖREN, Yünsa Yünlü San. ve Tic. A.Ş.

Sacit ERTAŞ, Erak Giyim San. ve Tic. A.Ş.

Urs Flach, Rieter Machine Works Ltd

Gülay GÖKBAYRAK, The Woolmark Company

Refik GÜLBAHAR, Denge Kimya ve Tekstil San. Tic. A.Ş.

Sabri İLKNUR, Asteks Kauçuk ve Plastik San. Tic. A.Ş.

Aşkın KANDİL, İpekiş Mensucat Türk A.Ş.

Ali Osman KİLİTÇİOĞLU, Altınyıldız Tekstil ve Konfeksiyon A.Ş.

Erdem KURGUN, Fourkim Tekstil Boya ve Kimya Ürünleri San. Tic. A.Ş.

Adem KURUCU, Şark Mensucat Fabrikası A.Ş.

Ebru MANAV AKYAR, Terra Analiz ve Ölçüm Cihazları Tic. A.Ş.

Doç. Dr. Serkan NOHUT, Selçuk İplik Sanayi ve Ticaret AŞ (Kara Holding)

Fatma ŞENER, SETAŞ Kimya San. A.Ş.

Dr. Ahmet TEMİROĞLU, Özen Mensucat Boya Terbiye İşletmeleri A.Ş.

Mahir TORSUN, Kadifeteks Mensucat San. A.Ş.

Sabri ÜNLÜTÜRK, Sun Tekstil A.Ş.

* *Alphatically Sorted by last name*



Scientific Committee*

- Prof. Dr. **Saber BEN ABDESSALEM** University of Monastir, Engineering School of Monastir (ENIM), Tunisia
- Prof. Dr. **Ashwini Kumar AGRAWAL** Indian Institute of Technology Delhi, Department of Textile Technology, India
- Prof. Dr. **Aysun AKŞİT** Dokuz Eylül University, Textile Engineering Department, Turkey
- Prof. Dr. **Seyed Hossein AMIRSHAHI** Amirkabir University of Technology (Tehran Polytechnic), Department of Textile Engineering, Iran
- Prof. Dr. **Pervin ANIŞ** Uludağ University, Textile Engineering Department, Turkey
- Prof. Dr. **Ozan AVİNÇ** Pamukkale University, Textile Engineering Department, Turkey
- Prof. Dr. **Ray H. BAUGHMAN** The University of Texas at Dallas, Nanotech Institute, USA
- Prof. Dr. **Ömer Berk BERKALP** İstanbul Technical University, Faculty of Textile Technologies and Design, Turkey
- Prof. Dr. **Abdulkadir BİLİŞİK** Erciyes University, Textile Engineering Department, Turkey
- Prof. Dr. **Mustafa Nazmi ERCAN** İstanbul Aydın University, Textile Engineering Department, Turkey
- Prof. Dr. **Jelka GERŠAK** University of Maribor, Research and Innovation Center for Design and Clothing Science, Slovenia
- Prof. Dr. **Özer GÖKTEPE** Tekirdağ Namık Kemal University, Textile Engineering Department, Turkey
- Assoc. Prof. Dr. **Marianna Ágnes HALÁSZ** Budapest University of Technology and Economics, Department of Polymer Engineering, Hungary
- Prof. Dr. **Luboš HES** Technical University of Liberec, Faculty of Textile Engineering, Czechia
- Prof. Dr. **Yaming JIANG** Tianjin Polytechnic University, School of Textiles, China
- Prof. Dr. **Hüseyin KADOĞLU** Ege University, Textile Engineering Department, Turkey
- Prof. Dr. **Paul KIEKENS** Ghent University, Department of Materials, Textiles and Chemical Engineering, Belgium
- Prof. Dr. **Vladan KONCAR** University of Lille, ENSAIT, Gemtex Textile Research Laboratory, France
- Prof. Dr. **Yasemin KORKMAZ** Kahramanmaraş Sütçü İmam University, Textile Engineering Department, Turkey
- Prof. Dr. **Seon Jeong KIM**, National CRI Center for Self-Powered Actuation, Hanyang University, Korea
- Prof. Dr. **Long LIN** University of Leeds, Department of Colour Science, UK
- Prof. Dr. **Carmen LOGHIN** Gheorghe Asachi Technical University of Iasi, Faculty of Textiles, Leather and Industrial Management, Romania
- Prof. Dr. **Koji NAKANE**, University of Fukui, Faculty of Frontier Fiber Technology and Science, Japan
- Prof. Dr. **R. Tuğrul OĞULATA** Çukurova University, Textile Engineering Department, Turkey
- Prof. Dr. **Hikmet Ziya ÖZEK** Tekirdağ Namık Kemal University, Textile Engineering Department, Turkey
- Prof. Dr. **Yiping QIU** Donghua University, College of Textiles, China



Prof. Dr. **Stephen RUSSELL** University of Leeds, Textile Materials and Technology Division, School of Design, UK

Prof. Dr. **Renzo SHAMEY** North Carolina State University, College of Textiles, USA

Prof. Dr. **Elias SIORES** University of Bolton, Institute for Materials, Research and Innovation, UK

Assoc. Prof. Dr. **António Pedro Garcia Valadares SOUTO** Minho University, Textile Engineering Department, Portugal

Prof. Dr. **Sachiko SUKIGARA** Kyoto Institute of Technology, Department of Fiber Science and Engineering, Japan

Prof. Dr. **Mehmet TOPALBEKİROĞLU** Gaziantep University, Textile Engineering Department, Turkey

Prof. Dr. **İsmail USTA** Marmara University, Textile Engineering Department, Turkey

Prof. Dr. **Savvas VASSILIADIS** Piraeus University of Applied Sciences, Department of Electronics Engineering, Greece

Prof. Dr. **Xungai WANG** Deakin University, Institute for Frontier Materials, Australia

* *Alphatically Sorted by last name*

NUMERICAL AND EXPERIMENTAL ANALYSIS OF WOVEN FABRIC IN OUT-OF-CENTER TENSILE LOADING

Ž. Šomodžić¹, S. Brnada^{1*}, E. Zdraveva¹ and S. Kovačević¹

¹University of Zagreb, Faculty of Textile Technology, Prilaz baruna Filipovića 28a, 10000 Zagreb, Croatia

*sbrnada@tff.hr

Abstract

Tensile response of a given material is recorded by the standard test in which the stress caused by the mechanical loading is evenly distributed in the test specimen. Textile materials are flexible and unable to withstand any in-plane compression. Compressive cut off can be viewed as the first source of the nonlinearity in textile deformation.

This paper brings the study in which these nonlinear phenomena are illustrated on the case of the out-of-centre tensile load in the modified standard tension test, where the force is applied to the specimen via the rigid crossbar. If the negative stress of bending part surpasses the average tensile stress, compressive cut off takes place and the static conditions must be satisfied in the new situation of a reduced specimen.

Key Terms

Tensile testing, eccentric loading, woven fabric, numerical analysis

1. Introduction

In an out-of-center or eccentric axial loading the force is applied to a material at a distance from the material center. In tensile testing such condition results in certain phenomena which differ depending on the type of materials tested. Searched literature dealing with the forth-mentioned condition in tensile testing mostly concerns composite materials based on concrete or epoxy resin matrices thus materials used in automotive, aerospace or civil engineering applications.

In a study of carbon fiber reinforced polymer (CFRP) confined concrete columns the authors have suggested a new stress-strain model considering load eccentricity. Increased in stiffness stress-strain relation resulted from the increase in the out-of-center loadings, while compared to concentric loaded columns, these columns showed 50 % higher ultimate failure strain¹. Another study considered woven glass fiber reinforced polyester resin (GFRP) composites and evaluation of their mechanical behaviour under monotonic or combined (tension/bending) loading. In the latter the specimens were mounted eccentrically thus the eccentric tension load was carried by offset steel shims. Initial non-linear load-displacement curve is associated with the high initial eccentricity, followed by a linear behaviour up to failure. The increase in the initial eccentricity results in decrease of the max tensile loads and its effect is more significant in case of the [0]₈ samples than the quasi-isotropic woven GFRP laminate [0/±45/90]_s². Compression axial and eccentric loading was applied to standard thin-walled column structure CFRP laminates with 8 plies symmetric to the mid-plane of the laminate. The authors have suggested the significance of the eccentric load on the column buckling depending on the eccentricity direction. The significance was further confirmed for the laminate ply orientation on the load critical values³. Other studies considering eccentricity were involved in the analysis of modified compact tension tests of cementitious materials⁴, compression tests of steel-fiber reinforced composite bars (SFCB)⁵ etc. Generally, the discussed findings are of paramount importance in the design of load bearing engineering constructions.

To the best of knowledge, analysis of similar kind i.e. out-of-center tensile loading and resulting phenomena in woven fabrics, are none in the searched literature. This study discusses

both experimental test and theoretically predicted model that describes the eccentric tensile load behaviour of woven rectangular strip fabric. Within this respect the study brings a novel research in the mechanics of textile materials.

2. Out-of-centre tension of woven fabric – a theoretical model

Consider the textile specimen in the form of a rectangular strip subjected to tensile load via the rigid crossbar attached to it at the lower end, see fig. 1a. In the present model let the material be assumed as linearly elastic but only in the tensile range, while in the compression it has virtually zero stiffness (it is flexible and buckles easily – “tension only” material). The adopted stress – strain diagram is shown in fig. 1b.

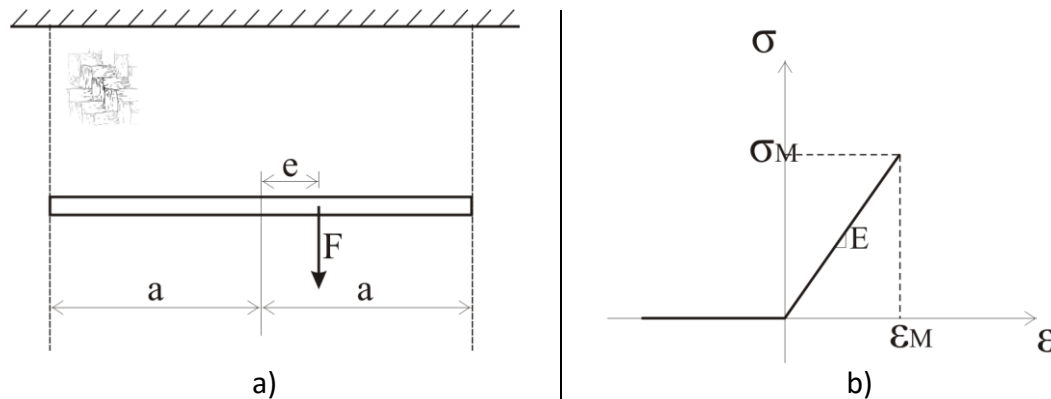


Figure 1. Specimen in tensile loading (a), and assumed stress – strain diagram (b)

Let us start the analysis by considering the following question: express the maximum stress in the specimen in terms of the force F and the geometry of fig. 1a. Let the half width of the specimen and the eccentricity of the loading be denoted by a and e respectively, see fig. 1a. Let also t and l denote the thickness and the length of the specimen respectively. Obviously, at $e=0$ the state of the specimen can be considered as uniform uniaxial stress (here we ignore the effect of boundary constraint of the lateral contraction). At $e>0$ the load can be considered as combination of pure tension and pure bending, and the corresponding displacement of the crossbar consists of the translation due to elongation and of the rotation due to bending. Stresses due to tensile and bending loads are

$$\sigma_t = \frac{F}{A} = \frac{F}{2at} \quad \sigma_{flex}^{max} = \frac{M}{W} = \frac{F \cdot e}{\frac{t \cdot (2a)^2}{6}} = \frac{3}{2} \frac{F}{a^2 t} e \quad (1)$$

The extreme stresses at the sides of the specimen are then by superposition

$$\sigma_{max} = \frac{F}{2at} \left(1 + 3 \frac{e}{a}\right) \quad \sigma_{min} = \frac{F}{2at} \left(1 - 3 \frac{e}{a}\right) \quad (2)$$

The corresponding linear distribution of stress in the cross section of the specimen is depicted in fig. 2a. This holds however only as long as the minimum stress remains positive. The limiting case of $\sigma_{min}=0$ and accordingly $e=a/3$ is shown in fig. 2b. With further increase of the eccentricity e , i.e. at $e>a/3$, the left part of the specimen undergoes negative (compressive) deformation and due to the compressive cut-off in the stress – strain diagram only the reduced portion of the cross section remains active in carrying the load, see fig. 2c.

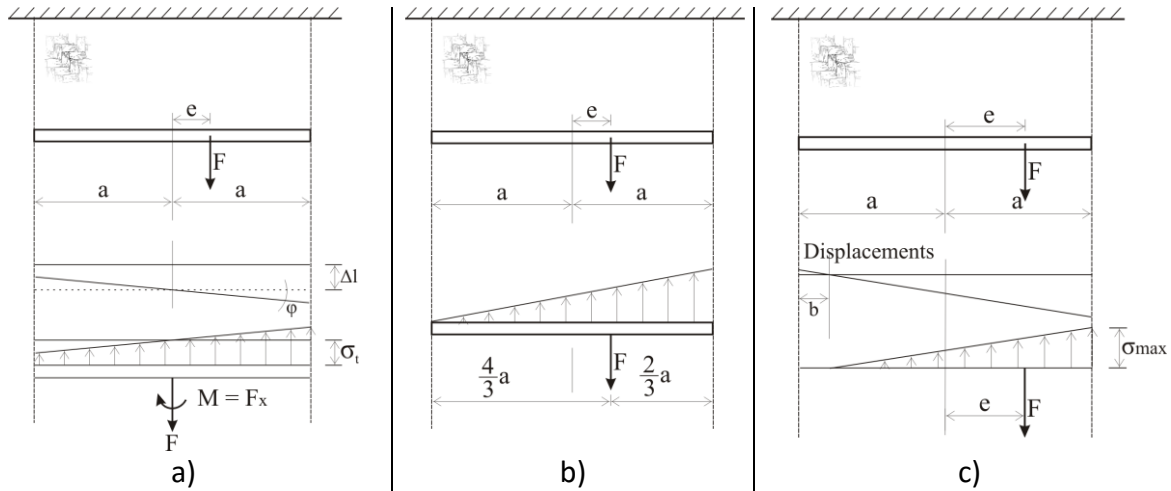


Figure 2. Stress distributions in the specimen in the cases: $e < a/3$ (a), $e = a/3$ (b) and $e > a/3$ (c)

In this latter case of fig. 2c the maximum stress is evaluated as follows: if the width of the non-carrying portion is denoted by b (fig. 2c), simple geometric consideration shows that the eccentricity e with respect to the whole specimen corresponds to reduced eccentricity with respect to the carrying portion $e' = e - b/2$. The condition of equality of medium stress (tensile part of stress) and maximum bending stress in the reduced carrying portion then leads to the expression for b :

$$\sigma_{med} = \frac{F}{(2a - b)t} = \sigma_{flex}^{max} = \frac{F(e - \frac{b}{2})}{t \frac{(2a - b)^2}{6}} \quad 1 = \frac{e - \frac{b}{2}}{\frac{2a - b}{6}}, \quad b = 3e - a \quad (3)$$

Finally, the expression for maximum stress in the specimen is obtained in the form

$$\sigma_{max} = 2\sigma_{med} = \frac{2F}{(2a - 3e + a)t} = \frac{2F}{3(a - e)t} \quad (4)$$

Values of the computed maximum stress for three specific values of load eccentricity e are obtained from (4) as follows:

$$e = \frac{1}{2}a \rightarrow \sigma_{max} = \frac{4F}{3at} \quad e = \frac{2}{3}a \rightarrow \sigma_{max} = 2 \frac{F}{at} \quad e = \frac{5}{6}a \rightarrow \sigma_{max} = 4 \frac{F}{at} \quad (5)$$

Dependence of maximum stress on the load eccentricity e for the given constant value of force F is shown in the diagram of fig. 3. Note that in the diagram linear law (2) and nonlinear law (4) meet at the transition point $e = a/3$.

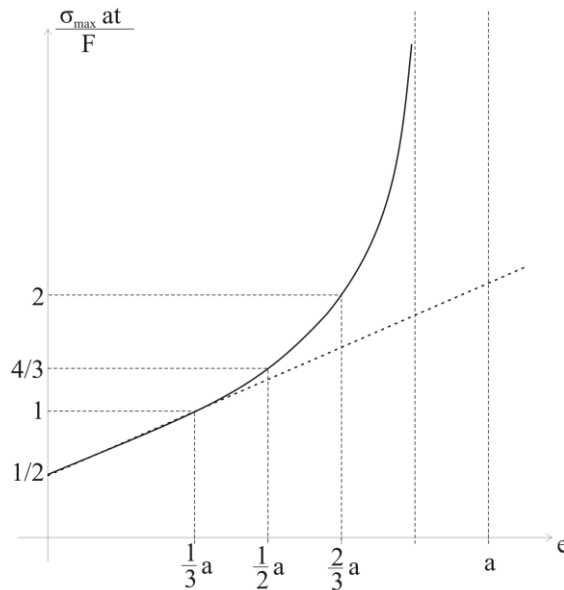


Figure 3. Diagram of maximum stress in terms of load eccentricity

Now let us consider the next question: if the tensile test on the fabric specimen were to be carried out with certain given eccentricity in the load application, how would that eccentricity alter the outcome of the test? Two main results of the test – Young’s modulus E and breaking force F_B would appear lower than for the “clean” test without eccentricity, and we aim to computationally predict that apparent reduction in stiffness and strength. One may consider that while the properties recorded by usual test where stress is uniform (fig. 1b) are pure material properties, the “apparent” properties in the case of out-of-centre load are joint material – geometric, or in other words structural properties. So let the Young’s modulus and breaking force recorded in the test with out-of-centre load be referred to as apparent modulus E^* and apparent breaking force F_B^* .

Consider first the transition case between full and partial loading of the specimen, fig.2b. Bending moment is $M=Fe=Fa/3$ and the angle of rotation of the bar due to bending of the specimen is

$$\varphi = \frac{Ml}{EI} = \frac{Ml}{E \frac{t \cdot (2a)^3}{12}} = \frac{3}{2} \frac{Ml}{Eta^3} \quad (6)$$

The displacement of the point of application of the force, or the apparent elongation of the specimen is then

$$\Delta l = \varphi \cdot (a + e) = \varphi \cdot \frac{4}{3} a = \frac{3}{2} \frac{Ml}{Eta^3} \cdot \frac{4}{3} a = \frac{2}{3} \frac{Fl}{Eta} \quad (7)$$

By analogy with Hooke’s law, the apparent Young’s modulus is obtained from the apparent stress and strain

$$\varepsilon^* = \frac{\Delta l}{l} = \frac{2}{3} \frac{F}{Eta} \quad E^* = \frac{\sigma^*}{\varepsilon^*} = \frac{\frac{F}{2at}}{\frac{2}{3} \cdot \frac{F}{Eta}} = \frac{3}{4} E \quad (8)$$

As for the apparent breaking force, it corresponds to the case when the maximum stress becomes equal to the ultimate stress of the material:

$$\sigma_{max} = \frac{F}{at} \quad \frac{F_B^*}{at} = \frac{F_B}{2at} \Rightarrow F_B^* = \frac{1}{2} F_B \quad (9)$$

So in this case the modulus appears reduced by a quarter, while the strength appears reduced to half.

Generally in the case of low eccentricity $e < a/3$ (fig. 2a), expressions (2) lead to conclusion that the breaking force is reduced by

$$F_B^* = \frac{F_B}{1 + 3 \frac{e}{a}} \quad (10)$$

The analysis of elongation (displacement of the point of force application) shows that the apparent elongation can be expressed as

$$\Delta l^* = \frac{Fl}{2atE} + \frac{3Fe^2l}{2Eta^3} = \frac{Fl}{2atE} \left(1 + 3 \left(\frac{e}{a} \right)^2 \right) \quad (11)$$

This means that the reduction of the apparent tensile modulus is given by the expression

$$E^* = \frac{E}{1 + 3 \left(\frac{e}{a} \right)^2} \quad (12)$$

The result (8) is confirmed if $e=a/3$ is introduced into (12). For example in the case $e=a/6$ expression (12) gives the apparent modulus reduced to $E^*=12E/13=0.923E$.

Finally, in the case of high eccentricity ($e > a/3$, fig. 2c) the bending moment on the carrying portion of the specimen is

$$M = F \left(e - \frac{b}{2} \right) = F \frac{a - e}{2} \quad (13)$$

and the angle of rotation of the bar due to bending is

$$\varphi = \frac{Ml}{EI} = \frac{F(a - e)l}{2Et \frac{(2a - b)^3}{12}} = \frac{2}{9} \frac{Fl}{Et(a - e)^2} \quad (14)$$

This produces the displacement, or the apparent elongation

$$\Delta l = \varphi(a - b + e) = \varphi \cdot 2(a - e) = \frac{4}{9} \frac{Fl}{Et(a - e)} \quad (15)$$

So in this case the apparent modulus takes the form

$$E^* = \frac{\sigma^*}{\varepsilon^*} = \frac{\frac{F}{2at}}{\frac{4}{9} \cdot \frac{Fl}{Et(a - e)}} = \frac{9}{8} E \frac{a - e}{a} \quad (16)$$

Again, (8) is confirmed if $e=a/3$ is introduced in (16). As for the apparent breaking force, due to expression (4) it takes the form

$$F_B^* = \frac{3}{4} F_B \frac{a - e}{a} \quad (17)$$

Three specific values of eccentricity e again give the corresponding stiffness and strength from (16) and (17) as follows. For $e=a/2$: $E^*=9E/16$, $F_B^*=3F_B/8$; for $e=2a/3$: $E^*=3E/8$, $F_B^*=F_B/4$; and for $e=5a/6$: $E^*=3E/16$, $F_B^*=F_B/8$. Note that here the apparent modulus and the breaking force are reduced proportionally, so for all values of $e > a/3$ the specimen reaches the break point at the same elongation. The theoretically predicted tensile diagrams with eccentricities are shown in figure 4.

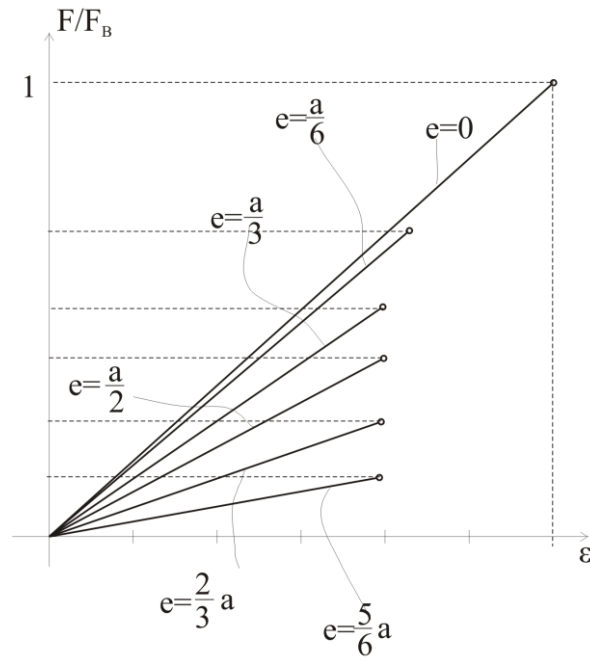


Figure 4. Theoretically predicted tensile diagrams with load eccentricity

3. Experiment

Testing of tensile and breaking properties of woven fabrics in the warp direction was carried out on the tensile tester. Woven fabric samples were made of 100 % cotton yarn, in a plain weave and fabric density of 20 yarns / cm in both directions. The tested samples dimensions were 350 mm x 50 mm. For the purpose of imposing out-of-centre tensile load, an additional clamp was used, which was axially connected to the non-elastic tape placed in the upper clamp of the tensile tester. Placing the woven fabric sample in an additional clamp in such a way that the chain grip is in a position different from the centre of the sample, respectively 0.0, 0.5, 1.0, 1.5 and 2.0 cm from the sample central axis, eccentricity is achieved. The samples were tested at a speed of 100 mm / min and the distance between the clamps was 200 mm.

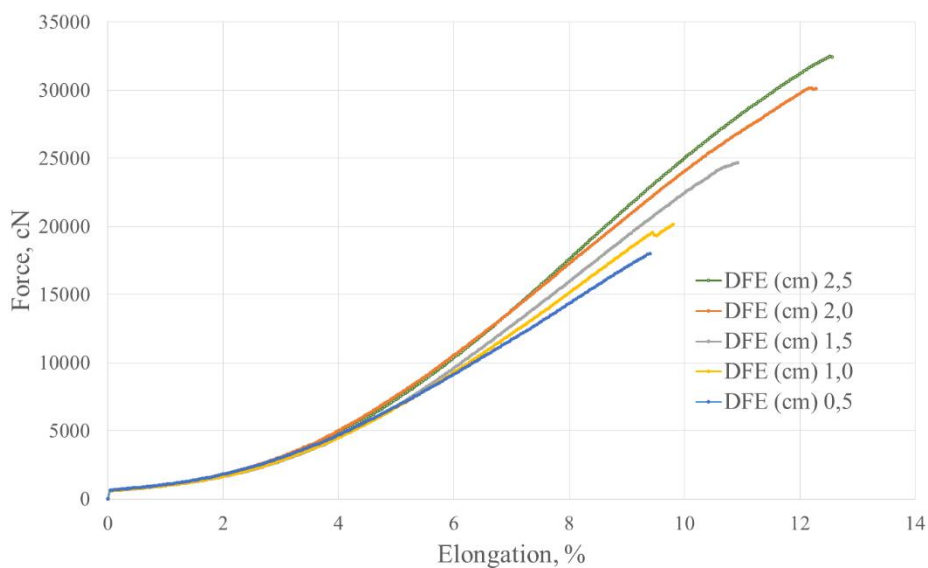


Figure 5. Tensile test curves with variation of force eccentricity

Figure 5 shows the stress-strain diagram of the woven fabric loaded with the tensile force, which is applied to the specimen via the rigid crossbar. DFE (cm) 2.5 line represents stress – strain curve of the specimen loaded in a non-eccentric way, where 2.5 stands for 2.5 cm from the edge of the specimen which is exactly the centre of the sample. Other stress – strain curves represent eccentrically loaded specimens with: 2.0, 1.5, 1.0 and 0.5 cm from the edge of the specimen, respectively. If the negative stress of the bending part surpasses the average tensile stress, compressive cut off takes place and the static conditions must be satisfied in the new situation of a reduced specimen. This results in the apparent reduction of the specimen strength and stiffness which is visible in Figure 5.

4. Conclusion

Nonlinear phenomena of woven fabric tensile behaviour are illustrated on the case of the out-of-centre tensile load in the modified standard tension test, where the force is applied to the specimen via the rigid crossbar. In the advanced strength of materials of solids, the case is regarded as the superposition of pure tension and pure bending. However, if the negative stress of bending part surpasses the average tensile stress, compressive cut off takes place and the static conditions must be satisfied in the new situation of a reduced specimen. This results in the nonlinear structural behaviour and in the apparent reduction of the specimen strength and stiffness.

In the future research, the analysis will be done for the case of material of woven fabric type, where the linear elastic law in tensile deformation is replaced by some more realistic nonlinear approximation. This is expected to require more effort in the computational description and analysis.

The rough initial computational results based on linear tensile law indicate similarity with experimental evidence of out-of-centre tensile test.

Acknowledgments

This work has been fully supported by the Croatian Science Foundation under the project number IP-2018-01-3170

References

1. Wu, Y.; Jiang, C. *Composite materials* **2013**, *98*, 228-241.
2. Khashaba, U. A.; Aldousari, S. M.; Najjar, I. M. R. *Journal of Composite Materials* **2012**, *46* (11), 1345-1355.
3. Wysmulski, P.; Debski, H. *Applied Composite Materials* **2018**, <https://doi.org/10.1007/s10443-018-9743-8>
4. Seitzl, S.; Rios, J. D.; Cifuentes, H.; Vesely, V. *Solid State Phenomena* **2017**, *258*, 518-521.
5. Tang, Y.; Sun, Z.; Wu, G. *Sustainability* **2019**, *11*, 1118-1133.